Printed Chipless Antenna as Flexible Temperature Sensor

Mitradip Bhattacharjee, *Member, IEEE*, Fatemeh Nikbakhtnasrabadi, *Graduate Student Member, IEEE*, and Ravinder Dahiya, *Fellow, IEEE*

***Abstract*—The ever-increasing number of devices on wearable and portable systems comes with challenges such as integration complexity, higher power requirements, and less user comfort. In this regard, the development of multifunctional devices could help immensely as they will provide the same functionalities with lesser number of devices. Herein, we present a dual-function flexible loop antenna printed on polyvinyl chloride (PVC) substrate. With a poly(3,4-ethylenedioxythiophene): polystyrene (PEDOT:PSS) section as part of the printed structure, the presented antenna can also serve as a temperature sensor by means of change in resistance. The antenna resonates at 1.2- and 5.8-GHz frequencies. The ohmic resistance of the temperature sensing part decreases by ∼70% when the temperature increases from 25 °C to 90 °C. The developed antenna was characterized using a vector network analyzer (VNA) in the same temperature range and the S11 magnitude was found to change by ∼3.5 dB. The induced current was also measured in the GSM frequency range and sensitivity of ∼1.2%/°C was observed for the sensing antenna. The flexible antenna was also evaluated in lateral and cross-bending conditions and the response was found to be stable for the cross-bending. Due to these unique features, the presented antenna sensor could play a vital role in the drive toward ubiquitous sensing through wearables, smart labels, and the Internet of Things (IoT).**

***Index Terms*—Flexible electronics, Internet of Things (IoT), poly(3,4-ethylenedioxythiophene): polystyrene (PEDOT:PSS), printed electronics, sensing antenna, temperature sensor.**

I. Introduction

ELECTRONIC research in recent years has seen a major focus toward the development of flexible printed devices that could confirm curvy surfaces and hence, meet the requirement of many applications, such as e-organs, robotics, wearable systems, Internet-of-Things (IoT) interfaces, etc., [1]–[3]. These advances have enriched the quality and quantity of data, for example, by allowing the use of sensors and electronic devices in locations where conventional planar electronics could not reach. This also means a dramatic increase in the number of sensing, computing, and communication devices, which comes with challenges such as complex integration and the need for more power or energy-efficient devices. In applications such as wearable systems, the increasing number of devices could be detrimental as it comes at the cost of user comfort. In this regard, the development of multifunctional devices will immensely help, as even with lower numbers they could provide the same level of functionality or richer data. In this regard, the devices such as antennas, which are typically used for wireless communication and power [4], [5], could offer an attractive route forward. Utilizing antennas as sensors is an interesting approach [6], as the concept can minimize the number of passive components and could lead to low-power solutions suitable for IoT applications in fields, such as healthcare, logistics, etc.

Herein, we present a dual function printed loop antenna which, in addition to typical communication function, could also serve as the temperature sensor. This study specifically addresses the issue of multipurpose electronic components. The sensing antenna presented in this work has a square loop pattern and realized by printing silver conductive paint on a 2.5 cm × 2.5 cm flexible polyvinyl chloride (PVC) substrate. The temperature-sensitive part was fabricated using conductive polymer PEDOT: PSS due to its excellent electrical property and stability. The device exhibits stable response under cross-bending condition, as discussed later. The presented temperature sensor antenna has also potential applications in smart packaging especially in food and logistic industries or water [7] (Fig. 1). The simple cost-effective fabrication technique used here makes the presented antenna sensor approach attractive for large-scale implementation. The presented antenna was characterized using a vector network analyzer (VNA) to measure the return loss (S11) at different temperatures. A theoretical study was also performed to calculate the induced current in the antenna and a comparison with the experimental result is presented. Furthermore, a comparative study was performed with a glass-based rigid antenna made of silver ink. The flexible antenna is found to be more efficient in terms of applicability and performance. In order to analyze the temperature sensing performance, the temperature-sensitive part was fabricated separately using silver electrodes and conductive polymer poly(3, 4-ethylenedioxythiophene): polystyrene (PEDOT:PSS)

Manuscript received July 7, 2020; revised October 26, 2020 and December 4, 2020; accepted January 9, 2021. Date of publication January 13, 2021; date of current version March 5, 2021. This work was supported in part by the Engineering and Physical Sciences Research Council (EPSRC) through Engineering Fellowship for Growth under Grant EP/R029644/1 and EU through North West Centre for Advanced Manufacturing Project under Grant H2020-Intereg-IVA5055 supported by INTERREG VA Programme and managed by the Special EU Programmes Body (SEUPB). *(Corresponding author: Ravinder Dahiya.)*

Mitradip Bhattacharjee is with the Bendable Electronics and Sensing Technologies Group, University of Glasgow, Glasgow G12 8QQ, U.K., and also with the Electrical Engineering and Computer Science, Indian Institute of Science Education and Research, Bhopal 462066, India.

Fatemeh Nikbakhtnasrabadi and Ravinder Dahiya are with the Bendable Electronics and Sensing Technologies Group, University of Glasgow, Glasgow G12 8QQ, U.K. (e-mail: ravinder.dahiya@glasgow.ac.uk).

Digital Object Identifier 10.1109/JIOT.2021.3051467

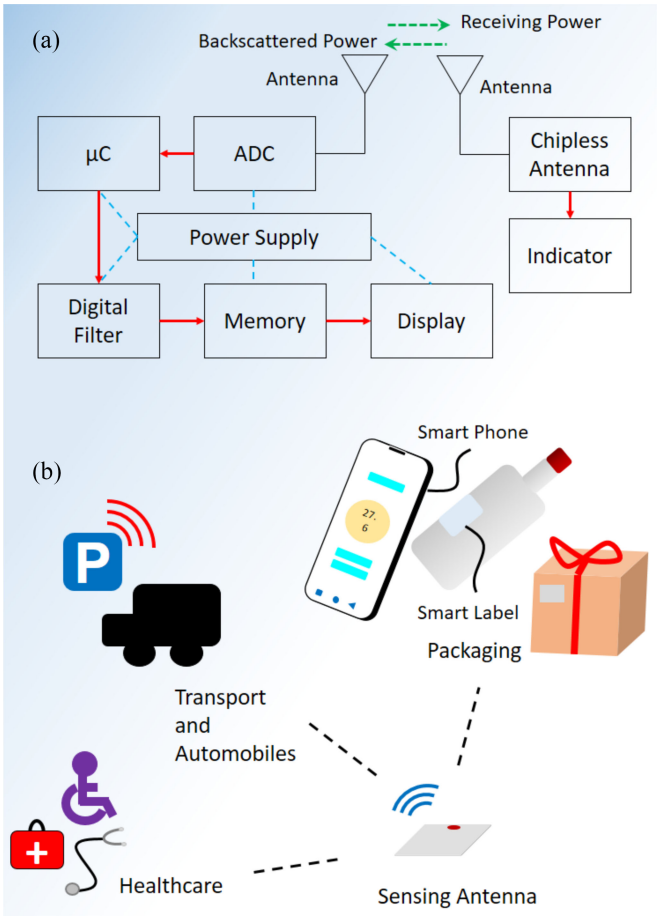

Fig. 1. (a) Schematic illustration of sensing antenna system. (b) Potential applications of sensing antennas.

and then the temperature sensing experiments were carried out. The presented sensing antenna is flexible and hence useful for wearables and similar applications. Furthermore, owing to materials used here, the sensing antenna is disposable and can possibly help to reduce electronic waste.

The remainder of this article is organized as follows. Section II presents the state of the art related to the reconfigurable sensing antenna. The materials employed in experiments, and fabrication and characterization methods are described in Section III. The fabricated antenna response is described in Section IV. Section V describes the performance of the temperature sensing part followed by the theoretical details regarding the antenna in Section VI. The results related to the sensing antenna are described in Section VII. Finally, the key outcomes are summarized in Section VIII.

II. State of the Art

Significant progress in printed electronics and nanotechnology has opened new avenues for using functional materials to develop sensing/electronic devices in flexible form factors and with wireless connectivity. These advances have allowed connecting different types of sensors to the cyberspace for applications, such as environment monitoring, wearable systems for health monitoring, and security [8]–[10]. Several types of sensors used in these application include sweat [11], temperature [12], strain [13], pH [14], radiation [15], volatile organic compounds [16], [17] and biomarkers for health [18], [19], environment, etc. A variety of flexible substrates has been used for the development of these sensors. In this direction, PVC is one of the most popular substrates for printed sensors due to its good thermal stability [14], [20], [22]. In parallel, the flexible or bendable antennas using a variety of materials has also been explored [23]–[26]. In particular, the antenna using printed sustainable materials is attractive [27], [28] as these could lead to disposable or reusable IoT hardware for the future. The trend thus far shows that the sensors and antenna are developed separately and integrated on the same or different substrates as per the requirements of target applications. Several prior works have demonstrated the use of wireless technology for the transmission of sensor data to portable devices such as smartphones [11]–[29]. In fact, such schemes have led to the emergence of new concepts such as mobile health and telerobotic [30]. But it is also clear that these schemes require an extra transmission antenna for communication, which leads to integration-related challenges. Thus, the use of an antenna as a sensor is gaining attention in recent days for IoT-based tags in multiple applications, such as electronic packaging, transportations, and healthcare. Using the same device for multiple functionalities is also an attractive solution for other emerging challenges such as the electronic waste.

Reconfigurable sensing antennas have emerged as a unique candidate for sensing solutions [31] and have attracted significant attention after the advent of IoT [32], [33]. Some of them include flexible antennas that are typically made of conductive inks/pastes and useful for applications such as wearable systems [34]–[38]. The conductive inks-based antennas do not offer a longer life span, which is acceptable for applications such as disposable smart labels or logos on the packaging. There are reports of sensing antennas having thermal switches. However, many of them are just capable of switching beyond a threshold temperature values [39]. Using the shift in frequency as a working principle, these antennas are less sensitive due to their wider bandwidth. They have been used for glucose, gas, and vapors sensing using the reflection loss as a sensing parameter [40], [41].

When it comes to temperature sensors, the conventional sensors are made of semiconductors [42], carbon derivatives [11]–[18], and temperature-sensitive metal-oxide composites [43] with sophisticated processing. These sensors are typically fabricated on hard substrates, which restrict their usability to applications where flexibility is not needed. Recently, the printed and flexible temperature sensor have also been explored for the use in biomedical and environmental applications [44]. The temperature-sensitive material plays an important role in deciding the performance of these device. A variety of materials, such as polyaniline, polystyrene, silicon, metal oxide, has been employed for resistive temperature sensors [45]. Among these, the conductive polymers have attracted significant attention owing to the ease of processing and good electrical properties. However, they suffer from low sustainability to temperature. In this regard, the PEDOT:PSS is attractive as it is most stable

TABLE I
COMPARISON OF THE PRESENTED SENSING ANTENNA WITH OTHER TEMPERATURE SENSING SYSTEMS

S.No	Active Material	Substrate	Range (°C)	Sensitivity (/°C)	Antenna	Ref
1	FGO–PVDF	PET	-10 – 30	-3.95×10^{-3}	NC	47
2	PEDOT: PSS-GO	Polyimide	RT – 100	1.09%	No	48
3	PEDOT: PSS/Ag	PET	20 – 70	0.8%	No	49
4	LEC	-	Temp. threshold	-	RC	51
5	tBA-co-PEGDMA	-	Temp. threshold	-	RC	50
6	PEDOT: PSS	PVC	25 – 90	1.2%	CL-SA	This Work

LEC: Liquid Elastomer Crystal, CL-SA: Chipless – Sensing Antenna, NC: NFC antenna with chip, RC: RFID antenna with chip.

conductive polymers and could lead to temperature sensors with high-temperature range [46]. Furthermore, their conductivity is tuneable, and this makes them attractive for sensing antenna. A few PEDOT:PSS composite-based temperature sensors [47]–[51] have been reported recently, but these either do not have a suitable range of operation for biomedical or smart packaging applications or are not suitable to be used as sensing antennas due to poor electrical behavior. There is hardly any flexible and chipless printed temperature sensing antenna reported so far. A comparison of temperature sensors and systems with the presented sensing antenna is shown in Table I.

III. METHODOLOGIES

A. Material

Commercial PVC sheet and Silver Conductive Paint (RS 186-3600) were procured from RS Components, U.K. PEDOT:PSS was procured from Sigma Aldrich, U.K. In this case, PEDOT:PSS was used as the active sensing material due to its electrical property and stability in ambient conditions.

B. Fabrication

The antenna was fabricated using conductive silver paint (RS 186-3600) on a commercial PVC substrate. Fig. 2(a) shows the schematic diagram of the antenna (only Ag ink) and the sensing antenna (PEDOT:PSS sensing element on the antenna). The PVC was cut into 2.5×2.5 cm pieces and a pattern was formed on the flexible PVC substrate using silver paste as illustrated Fig. 2(b). The length of each side of the square antenna was 2.5 cm with a conductive track width of 2 mm. The samples were then dried in a hot-air oven at 50 °C for 30 min. The antenna along the whole structure was fabricated using Ag ink. However, for a sensing antenna, a 2-mm gap was left in the middle of the antenna just opposite to the SMA (SubMiniature version A) connector (RS Components). The SMA connectors were connected using Ag paste and epoxy. Furthermore, a 10 μl PEDOT:PSS was dispensed in the 2-mm gap using a micropipette. The samples were further dried at 50 °C for 1 hr in an air oven. Thereafter, the samples were electrically characterized to check the response of the fabricated antennas.

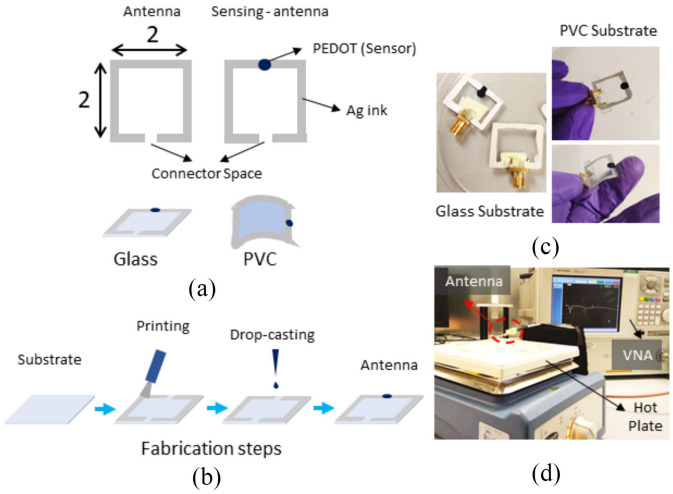

Fig. 2. (a) Schematic illustration of antenna design. (b) Fabrication steps. (c) Optical images of fabricated antennas on glass and PVC substrate. (d) Optical image of the experimental set up.

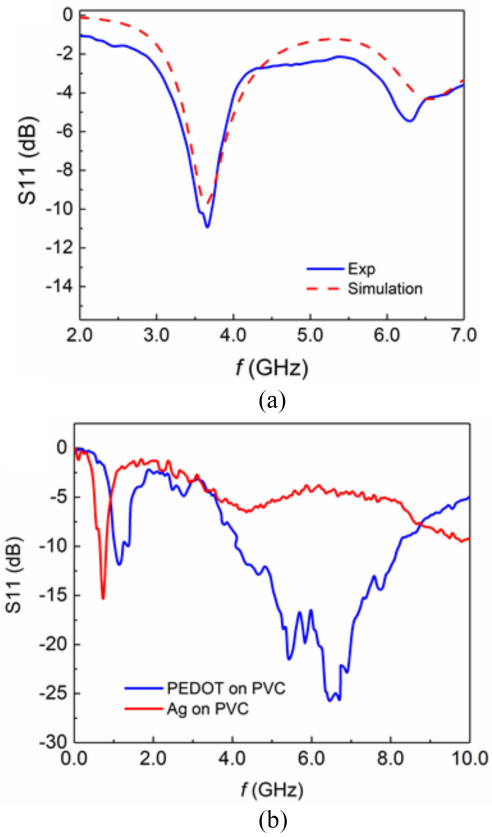

Fig. 3. (a) Response of glass substrate-based antenna (S11 value) and comparison of experiment (Exp) results and theoretical analysis (simulation). (b) Response of PVC substrate-based flexible antenna (Ag on PVC) and temperature sensing antenna (PEDOT on PVC).

C. Characterization

The experiment was carried out with a PNA vector network analyzer (VNA) (Agilent E83628). The sensors were first connected with SMA connectors and then connected with the probes of VNA. Prior to the measurement, open short load (OSL) calibration was performed with Keysight 85052D calibration kit. The S11 parameter or the return loss was

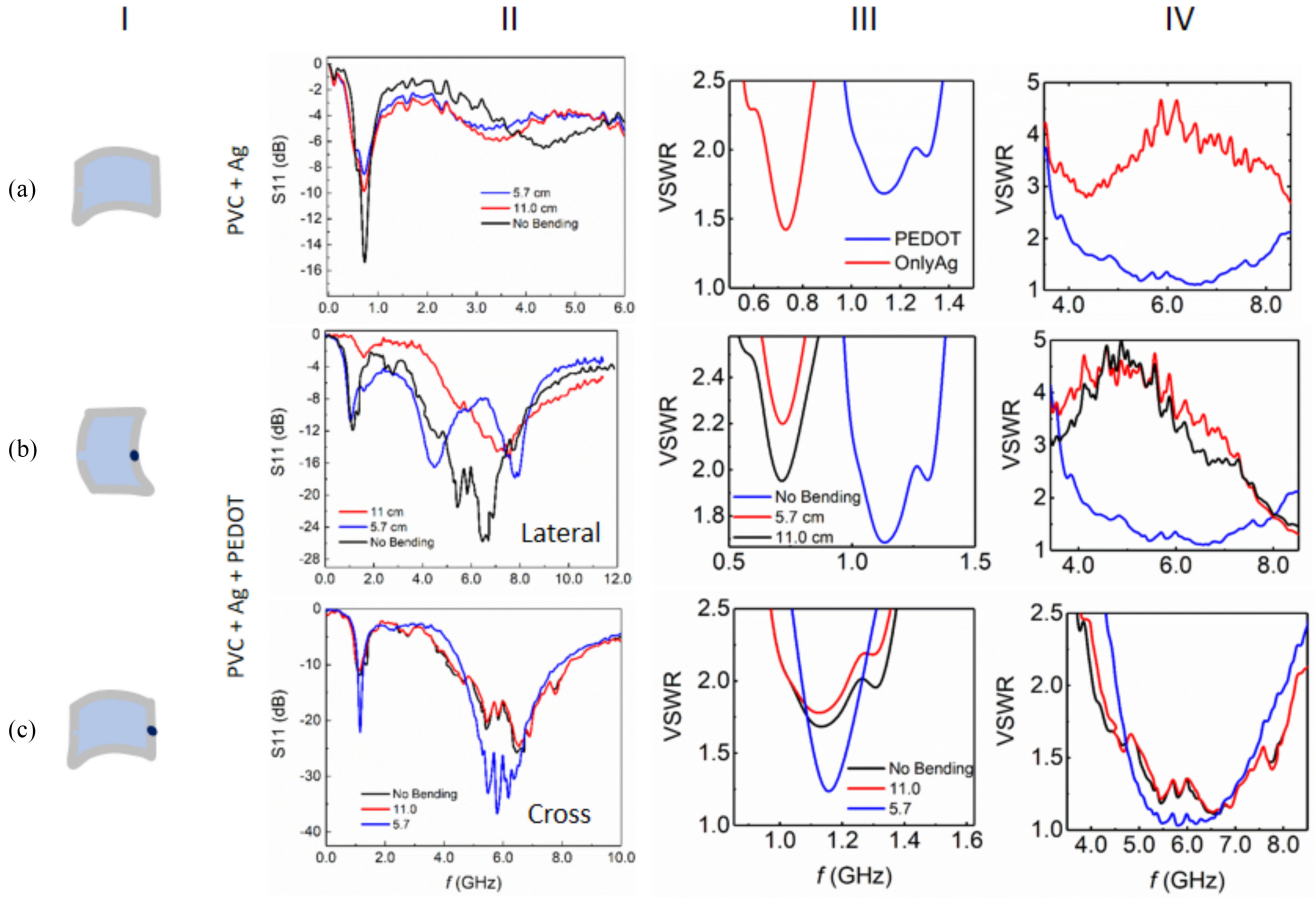

Fig. 4. Bending effect on fabricated sensing antenna and the corresponding VSWR values with and without PEDOT:PSS sensing material. Column I shows the schematic of sensing antenna in different bending conditions. (a) Bending of sample without PEDOT:PSS. (b) Lateral bending of sensing antenna. (c) Cross-bending of sensing antenna. Column II shows the respective S11 values and columns III and IV show the VSWR values (legends of column IV are the same as column III). The legends in the plots show the bending radii 11.0 and 5.7 cm.

analyzed for different sensing antennas. The temperature change experiments were performed using a temperature controllable hotplate (Stuart CD162). A high-precision IR thermometer (FLUKE 62 MAX) was used to monitor the temperature while performing the experiments. The sensing antenna was placed ∼2 cm above the hotplate so that the connector did not touch the heated surface as shown in Fig. 2(d). The experiments were performed at ambient conditions and the temperature of the probe was also monitored during the experiments. Thereafter, the temperature of the hotplate was increased to the desired value and the S11 parameter corresponding to that temperature was recorded. The actual temperature on the sensor was recorded using the IR thermometer.

IV. Antenna Response

Antenna design and computational analysis were performed using commercially available software HFSS and the results are compared with the experimental response. For biomedical sensing applications, the antennas are designed in the microwave range [40]. Hence, the initial experiments were started with an antenna on a glass substrate that was designed to resonate at ∼4 GHz. However, the flexible sensing antenna resonates at ∼1.2 and ∼5.8 GHz. Hence, it also works with mobile phone radiations at the GSM frequency range (900–1800 MHz). In this case, the GSM frequency was employed to get the induced current that acts as the sensing parameter in this study. Fig. 3(a) shows the comparison between experimental and simulated values of S11 parameters of loop antenna fabricated on a glass substrate using Ag ink. Fig. 3(b) shows the experimental values of S11 parameters for Ag-based antenna and sensing antenna having PEDOT:PSS on the PVC substrate. It was observed that PEDOT:PSS on the PVC substrate was suitable for temperature sensing. Hence, further experiments were carried out using this proposed antenna.

The fabricated flexible sensing antennas were further tested under bending conditions. In this regard, two types of antenna were employed: 1) Ag-based antenna on flexible PVC and 2) PEDOT:PSS-based sensing-antenna on flexible PVC substrate. Two types of bending conditions were taken under consideration: 1) lateral bending—where the sensing patch was bent during the bending and 2) cross-bending—where the bending does not affect the sensing material. Two bending radii, 5.7, and 11.0 cm, were employed in the experiments. The bending radii were decided based on the radii of disposable bottles used for water or beverages. Two different types of parameters were taken into consideration for each sample: 1) S11 parameter with bending of the sensing antenna and 2) voltage standing wave ratio (VSWR) parameters for

each case. Row A of Fig. 4 illustrates the schematic of flexible Ag antenna on PVC (column I), the S11 parameter with the frequency of the flexible Ag antenna upon different extent of bending (column II), comparison of VSWR values for Ag antenna (only Ag) and PEDOT:PSS-based sensing antenna (PEDOT) without bending condition at 0.5–1.5 GHz (column III) and 4–8 GHz (column IV) range. It is clear from the S11 and VSWR values in Row A that the sensing antenna has reasonable performance in both 0.5–1.5 GHz and 4–8 GHz range with resonant frequencies at ∼1.2 and ∼5.8 GHz. Further experiments were carried out for the PEDOT:PSS sensing antenna. Rows B and C show the effect of lateral and cross-bending in PEDOT:PSS sensing antenna, respectively. The later bending and cross-bending conditions are explained schematically in column I of rows A and B. Columns II–IV illustrate the change in the S11 parameter with frequency due to bending and the corresponding change in VSWR values at 0.5–1.5 GHz and 4–8-GHz frequency range, respectively, for rows B and C. The S11 and VSWR values in column I, II, and III of row B suggest that the lateral bending of the sensing antenna cause a significant shift in the operating frequency and this would not be desirable for the operation of the sensor. Moreover, the VSWR values of the sensor show the extent of reflection loss for the sensors. The performance of the sensing antenna was considerably good at 0.5–1.5-GHz range, the VSWR value reduced considerably upon lateral bending. However, the sensor showed a stable response in the case of cross-bending as illustrated in row C of Fig. 4. The VSWR value was close to 1 at 0.5–1.5-GHz range as shown in column IV of row C, and thus, it has the best performance at this frequency range. The sensing antenna was further tested for temperature sensing applications.

V. Temperature Sensing

PEDOT:PSS is sensitive to temperature and its rate of carrier mobility rises or its resistance decreases with increasing temperature [46]. The PEDOT:PSS element in the antenna was tested for temperature sensing. A temperature sensing sample was prepared separately on PVC substrate with PEDOT:PSS having two silver electrodes. The sensing sample was then characterized using LabVIEW-enabled digital multimeter and heating arrangement, i.e., a hotplate having digital display control, as described in Section III. The temperature-sensitive PEDOT:PSS with two Ag electrodes was placed on the digital hotplate and the temperature was varied from 25 ° C to 90 °C. The resistance decreased with the increase in temperature as illustrated in Fig. 5(a). The sensor was left to saturate before the temperature of the hotplate underneath was increased to the next higher value. The resistance decreases and reaches a stable state in around 8–12 s for a temperature increase of ∼5 °C from 30 °C to 35 °C, as shown in Fig. 5(b). Furthermore, the sensor was exposed to different temperatures, and the response (R/R_0) was recorded. Fig. 5(c) shows the change in R/R_0 with temperature and Fig. 5(d) shows the same for normalized conductance (σ/σ_0).

As the sensor is a part of the antenna, the conductance value is an important parameter for the induced current. In this case, the change in normalized conductance showed a nice quadratic

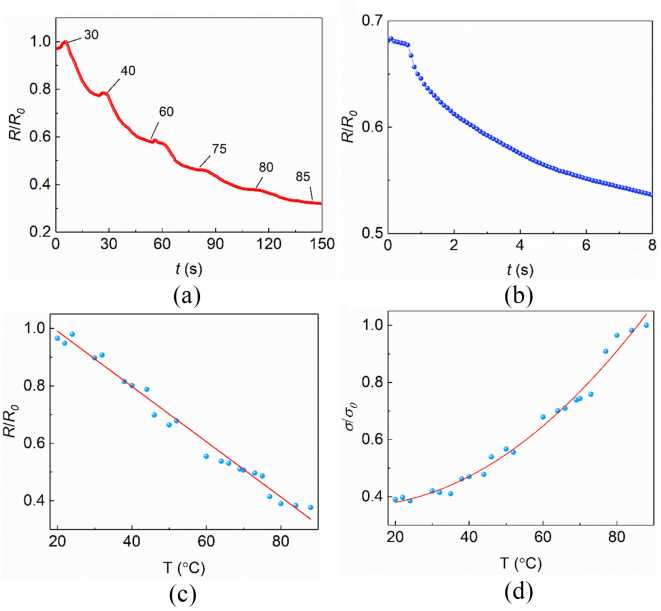

Fig. 5. (a) Change in normalized resistance with time. (b) Sensor response (R/R_0) for temperature increase of ∼5 °C, from 30 °C to 35 °C. (c) Response of sensor at different temperature (T). (d) Change in normalized conductance (σ/σ_0) with temperature.

fit with the variation in temperature. The dependence of conductance with temperature can be expressed as a second-order equation, $Y = ax^2 + bx + c$ as shown in Fig. 5(d), where $a = 1.1e-4$, $b = -2e-3$, and $c = 0.3$. In the literature also, a quadratic relation between resistance and temperature is reported [52], [53]. The relation between the parameters was further employed in the antenna model to calculate the induced current. However, the resistance, in this case, is linear with temperature $Y = mx + c'$, as shown in Fig. 3(c) where $m = 0.96e-3$ and $c' = 1.1$. The resistance changed by about 60 Ω for a change of temperature of 5 °C from 30 °C to 35 °C, while the noise is ∼2.7%, which was calculated by measuring the fluctuations of response from the linear fit and the temperature resolution, i.e., minimum difference between two detectable consecutive temperature values (calculated to be ∼2 °C).

VI. Antenna Details

In order to understand the induced current through the sensing antenna and the effect of the temperature on the same, a theoretical analysis [54], [55] was performed with small loop assumptions. The aim of this study was to calculate the average current in far-field through the antenna and hence, to see if the model works in the frequency range of interest. The equivalent circuit for a receiving antenna contains an open-circuit voltage V_{OC}, a load impedance Z_L, and an input impedance Z_a connected in series as illustrated in the inset of Fig. 6(a). The current flowing through the loop is related to V_{OC}. With these assumptions, the induced current I can be written as

$$I = \frac{V_{OC}}{Z_L + Z_a}. \tag{1}$$

The voltage developed across the open terminal of the loop can be explained by Faraday's law for the time-varying

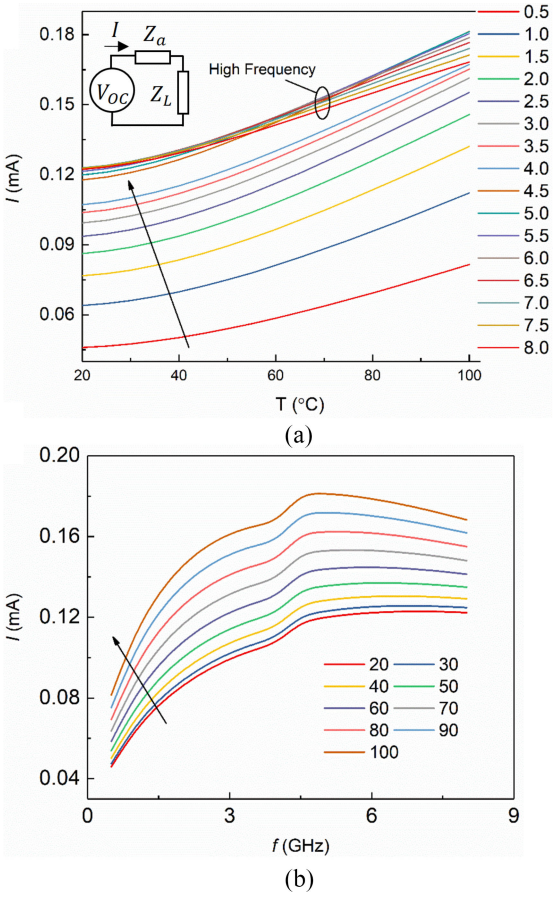

Fig. 6. Induced current values. (a) With temperature. (b) With frequency obtained from the theoretical study.

magnetic flux. For a loop having N turns, the voltage is

$$V_{OC} = -j\omega N \int\int \overline{B} \cdot d\overline{s} \tag{2}$$

where $\omega = 2\pi f$ is the radian frequency, $\overline{B}$ magnetic flux density through the loop, and $d\overline{s}$ is the incremental surface area of the loop. The direction of the area, in this case, is normal to the loop. Considering the loop to be small, the approximate magnetic flux crossing the loop is $\int\int \overline{B} \cdot d\overline{s} \approx B(\pi b^2)$, where B is the magnitude of magnetic flux. Moreover, the magnetic flux density can be calculated as $\overline{B} = \mu\overline{H}$, where $\mu = \mu_0\mu_r$ is the permeability of the material. ($\mu_0 = 4\pi \times 10^{-7}$ H/m, the permeability of free space and μ_r is the relative permeability of the material.) Hence, the induced voltage in an N turn small loop can be calculated as

$$V_{OC} = -j\omega N\pi b^2 \mu_0 \mu_r H. \tag{3}$$

The voltage across the Z_L can be calculated as

$$V_L = V_{OC}\frac{Z_L}{Z_a + Z_L}. \tag{4}$$

Whereas, the induced current is determined using the input impedance of the antenna, which is defined as $Z_a = R_a + jX_a$, where R_a is the input resistance, and X_a is the input reactance of the antenna. In addition, the input resistance also has two parts $R_a = R_r + R_\Omega$, where, R_r is the radiation resistance, and R_Ω is the ohmic resistance of the antenna. The radiation resistance of a small N-turn loop antenna is

$$R_r = 31200\left(\frac{N\pi b^2}{\lambda^2}\right)^2. \tag{5}$$

However, the ohmic resistance attributes to the power loss in terms of heating due to the current flow. If the conductivity of the material is σ, then the ohmic resistance (i.e., the surface resistance) for each turn is typically approximated as follows:

$$R_\Omega = \frac{b}{a}\sqrt{\frac{\omega\mu}{\sigma}} \tag{6}$$

where b is the radius of the loop and a is the radius of the wire. The small loops have high inductance, which can be calculated as

$$L = \mu bN^2\left(ln\left(\frac{8b}{a}\right) - 2\right). \tag{7}$$

In general, the reactance X_a is the inductance associated with the antenna. Hence, the input impedance can be written as

$$Z_a = R_a + j\omega\mu bN^2\left(ln\left(\frac{8b}{a}\right) - 2\right) = 31200\left(\frac{N\pi b^2}{\lambda^2}\right)^2 + \frac{b}{a}\sqrt{\frac{\omega\mu}{\sigma}} + j\omega\mu bN^2\left(ln\left(\frac{8b}{a}\right) - 2\right). \tag{8}$$

Hence, the current induced in the small loop can be calculated as

$$I = \frac{-j\omega N\pi b^2\mu_0\mu_r H}{Z_L + 31200\left(\frac{N\pi b^2}{\lambda^2}\right)^2 + \frac{b}{a}\sqrt{\frac{\omega\mu}{\sigma}} + j\omega\mu bN^2\left(ln\left(\frac{8b}{a}\right) - 2\right)}. \tag{9}$$

This equation describes the effect of the load impedance on the current in the loop. Fig. 6 shows the obtained current values with (A) temperature and (B) frequency. The plots suggest that induced current increases with temperature and has a higher influence in higher frequencies. However, Fig. 6(b) shows that the current also increases at low-frequency ranges. The experiments were performed with the sensing antenna as a receiver in the GSM range (900–1800 MHz) with mobile phone radiation to measure the induced current as discussed later. Before performing the tests using the mobile phone, the sensing characterization was performed for the printed sensing antennas using VNA and temperature arrangements.

VII. Temperature Sensing Antenna

The temperature sensing properties of the antenna were tested by increasing the temperature of the antenna using a controllable hotplate. The $S11$ parameter was measured for the sensing antenna at different temperature conditions. It was observed that the magnitude of return loss decreased due to the enhancement of temperature. This can be attributed to the change in the resistance of the sensing PEDOT:PSS element that leads to the overall change in the sensing antenna impedance. Fig. 7(a) and (b) shows the S11 parameter versus frequency for PEDOT:PSS sensing antenna at different temperatures ranging from 25 °C to 90 °C at 1–2.5 GHz and

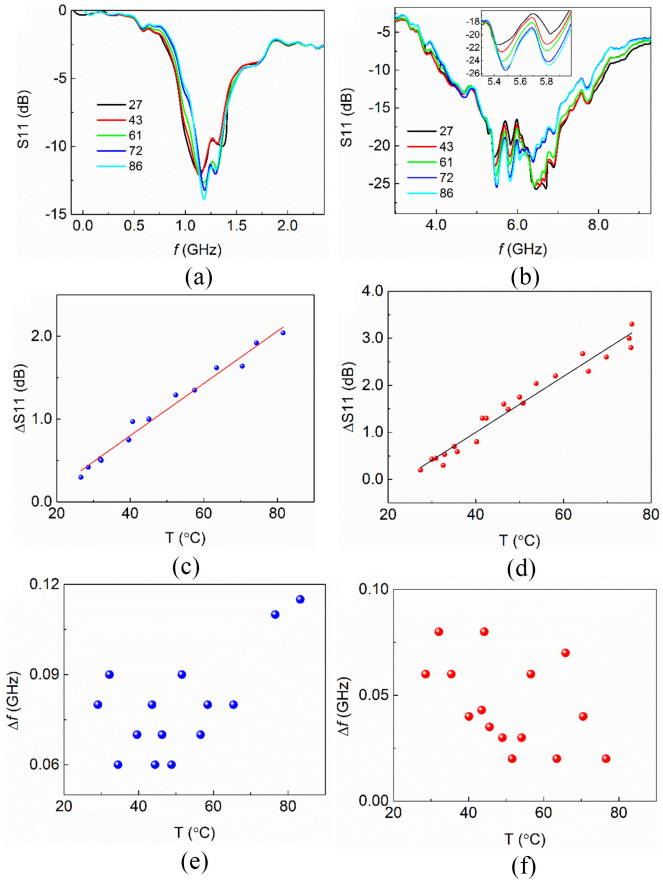

Fig. 7. Response of antenna at different temperatures. (a) and (b) S11 parameter analysis of antenna at 1–2.5 GHz and 5–6 GHz frequency range. (c) and (d) response (ΔS_{11}) at different temperatures for the above-mentioned frequency ranges, respectively. (e) and (f) show the frequency shifts due to the temperature changes for the above two frequency ranges, respectively.

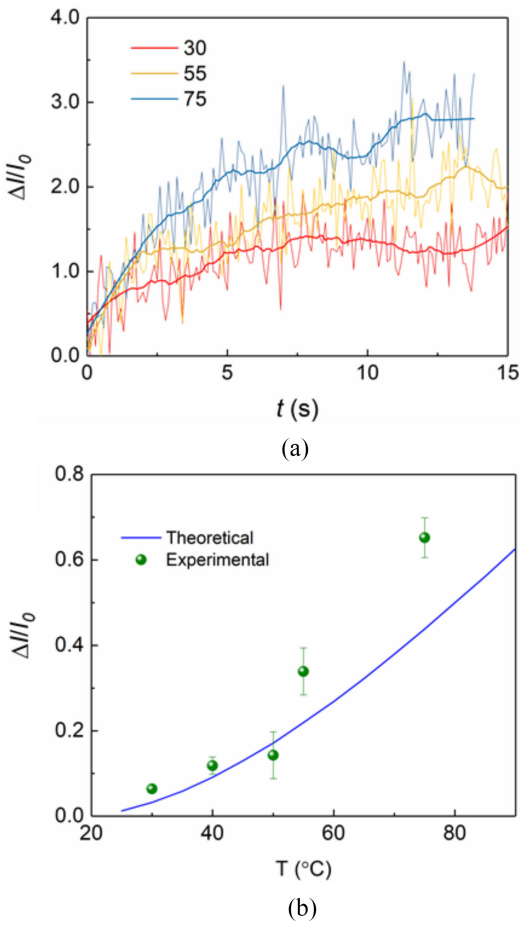

Fig. 8. (a) Response ($\Delta I/I_0$) of the temperature sensing antenna with time for different temperature values. (b) Comparison of the experimental and theoretical results of the temperature sensing antenna.

5–6 GHz frequency range, respectively. Fig. 7(c) and (d) shows the change in $S11$ parameter magnitude ($\Delta S11$) with temperature for the said frequency ranges, respectively. The shift in the frequency due to the temperature changes was also studied as illustrated in Fig. 7(e) and (f). The shift, in this case, was nominal and did not show any trend. Thus, the change in the $S11$ parameter ($\Delta S11$), which indicates the change in power, was more reliable for temperature detection. The sensors were calibrated so that the absolute temperature can be measured along with the change of the temperature. However, the same can also be achieved by integrating a reference sensing antenna in to the system.

The sensing antenna was further tested in the GSM range (900–1800 MHz). In this case, the sensing antenna was kept at ∼1 cm from a GSM mobile phone that was transmitting the RF signal and the rectified induced current was measured using a digital multimeter at different temperatures. The temperature was changed using the hotplate and an IR thermometer was employed to measure the temperature of the sensing antenna during the experiment. It was observed that the induced current was higher in the case of higher temperatures as predicted previously using the simulation. Fig. 8(a) shows the change in the current response ($\Delta I/I_0$) with time. Furthermore, the response was also compared with the simulation results and the experimental results were found to be at per with the simulation as shown in Fig. 8(b).

The idea of using the sensing antenna is to reduce the number of electronic components in a system and this is achieved through a multifunctional antenna. Although the proposed flexible sensing antenna showed an encouraging response in temperature sensing in the reported bending range, one of the major issues with this type of sensing antenna is the significant shift in the resonant frequency upon large bending. The effect of bending is significant for lateral bending condition as illustrated in Fig. 4. The simultaneous variation of bending and temperature could be handled by mathematical compensation with appropriate system design after modeling the same theoretically. Another solution for this issue would be a thicker substrate and stretchable inks that have stable electrical properties with stretching or bending. However, a thick substrate may restrict the bendability of the antenna, and thus, there exists a tradeoff between the substrate thickness and its bendability. The sensing antennas were found to be stable for 15–16 weeks after they were stored in ambient conditions. The effect of humidity was minimum as the sensor operates in 25 °C–90 °C and at high temperature, the adsorption of water was minimum. However, the stability of the sensing antenna can further be increased by using a thin transparent coating and proper storage.

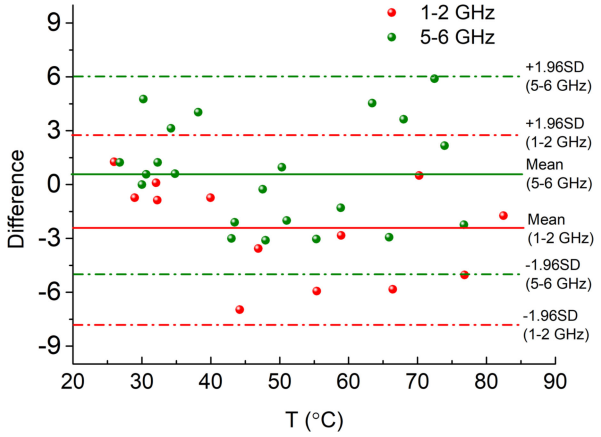

Fig. 9. Bland-Altman plot of the measured temperatures using the thermometer and the proposed temperature sensing antenna.

The performance of the sensing antenna was found to be superior compared to its counterparts as described in Table I. The sensor showed a maximum of 70% change in resistance for a temperature change of ∼60 °C for a temperature range from 25 °C to 90 °C. The antenna was found to be resonating at 1.2 and 5.8 GHz. The developed antenna was characterized using VNA in the above temperature range and a sensitivity of ∼1.2%/°C was observed. A maximum of ∼20% change in reflection loss was observed for 25 °C–90 °C temperature change at a frequency of ∼5.8 GHz. As a comparative study, the Bland-Altman plot of the measured temperatures using the thermometer and the proposed temperature sensing antenna is illustrated in Fig. 9. The plot shows that the measured values using the temperature sensing antennas are in the range of ±1.96SD (i.e., standard deviation).

VIII. Conclusion

In this article, PEDOT:PSS-based chipless printed loop antenna is presented for temperature sensing application. The antenna was fabricated in both glass and flexible PVC substrate. It was observed that the flexible PEDOT:PSS sensing antenna performance was better compared to the rigid glass-based antenna. A series of bending experiments was also carried out and the cross-bending condition was found to be suitable for the sensing applications. The temperature sensing part was fabricated separately and characterized at different temperatures from 25 °C to 90 °C. The sensor showed a maximum of 70% change in resistance for a temperature change of ∼60 °C. The temperature sensing was also characterized separately using a digital multimeter for a temperature range from 25 °C to 90 °C. The sensor showed a 70% change in resistance for a temperature change of ∼60 °C. A comparative study was performed with a glass-based rigid sensing antenna. However, the flexible sensing antenna was found to be more efficient in terms of applicability and performance. The antenna was found to be resonating at 1.2 and 5.8 GHz. The developed flexible antenna was further characterized using VNA in the temperature range of 25 °C–90 °C to measure the change in the S11 magnitude. A sensitivity of ∼1.2%/°C was observed for the sensing antenna. The antenna was found to be suitable for bending applications as well. It was also observed that the return loss and resonant frequency change significantly once the antenna undergoes a lateral bending. However, the antenna is found to be more stable in the case of cross-bending conditions. The value of VSWR was found to be satisfactory even in bending conditions. A maximum of ∼20% change in reflection loss was observed for a temperature change from 25 °C to 90 °C at a frequency of ∼5.8 GHz. This flexible sensing antenna can be used as temperature sensing applications in smart labels. Furthermore, the temperature sensing antenna could be integrated with clothes and potentially used for the measurement of body temperature to trace patients of infectious viral diseases such as COVID. With features, such as printability and disposability, the presented sensing antenna could provide an affordable solution for large-scale deployment. Future work will involve a detailed study on measurement of human body temperature.

Acknowledgment

The views and opinions in this document do not necessarily reflect those of the EU or the SEUPB.

References

[1] R. Dahiya, D. Akinwande, and J. S. Chang, "Flexible electronic skin: From humanoids to humans," *Proc. IEEE*, vol. 107, no. 10, pp. 2011–2015, Oct. 2019.
[2] W. Dang, V. Vinciguerra, L. Lorenzelli, and R. Dahiya, "Printable stretchable interconnects," *Flexible Printed Electron.*, vol. 2, Mar. 2017, Art. no. 013003.
[3] R. Dahiya *et al.*, "Large-area soft e-Skin: The challenges beyond sensor designs," *Proc. IEEE*, vol. 107, no. 10, pp. 2016–2033, Oct. 2019.
[4] K. S. Patil and E. Rufus, "A review on antennas for biomedical implants used for IoT based health care," *Sens. Rev.*, vol. 40, no. 2, pp. 273–280, 2019.
[5] A. A. Elijah and M. Mokayef, "Miniature microstrip antenna for IoT application," *Mater. Today Proc.*, vol. 29, pp. 43–47, Jan. 2020.
[6] C. Occhiuzzi, S. Caizzone, and G. Marrocco, "Passive UHF RFID antennas for sensing applications: Principles, methods, and classifcations," *IEEE Antennas Propag. Mag.*, vol. 55, no. 6, pp. 14–34, Dec. 2013.
[7] J. Shutler *et al.*, *Risk of SARS-CoV-2 Infection From Contaminated Water Systems*, medRxiv, Yale University, New Haven, CT, USA, 2020, doi: 10.1101/2020.06.17.20133504.
[8] E. S. Hosseini, M. Bhattacharjee, L. Manjakkal, and R. Dahiya, "Healing and monitoring of chronic wounds: Advances in wearable technologies," in *Digital Health: Exploring the Use and Integration of Wearables*, S. Stuart and A. Godfrey, Eds. London, U.K.: Academic, 2021.
[9] B. Ali and A. I. Awad, "Cyber and physical security vulnerability assessment for IoT-based smart homes," *Sensors*, vol. 18, no. 3, p. 817, 2018.
[10] L. Manjakkal, A. Pullanchiyodan, N. Yogeswaran, E. S. Hosseini, and R. Dahiya, "A wearable supercapacitor based on conductive PEDOT:PSS-coated cloth and a sweat electrolyte," *Adv. Mater.*, vol. 32, no. 24, 2020, Art. no. 1907254.
[11] W. Dang, L. Manjakkal, W. T. Navaraj, L. Lorenzelli, V. Vinciguerra, and R. Dahiya, "Stretchable wireless system for sweat pH monitoring," *Biosens. Bioelectron.*, vol. 107, pp. 192–202, Jun. 2018.
[12] M. Soni, M. Bhattacharjee, M. Ntagios, and R. Dahiya, "Printed temperature sensor based on PEDOT: PSS-graphene oxide composite," *IEEE Sensors J.*, vol. 20, no. 14, pp. 7525–7531, Jul. 2020.
[13] M. Bhattacharjee, M. Soni, P. Escobedo, and R. Dahiya, "PEDOT:PSS microchannel-based highly sensitive stretchable strain sensor," *Adv. Electron. Mater.*, vol. 6, no. 8, 2020, Art. no. 2000445.
[14] L. Manjakkal, W. Dang, N. Yogeswaran, and R. Dahiya, "Textile-based potentiometric electrochemical pH sensor for wearable applications," *Biosensors*, vol. 9, no. 1, p. 14, 2019.
[15] M. Zhang and J. T. W. Yeow, "A flexible, scalable, and self-powered mid-infrared detector based on transparent PEDOT: PSS/graphene composite," *Carbon*, vol. 156, pp. 339–345, Jan. 2020.

[16] M. Bhattacharjee, V. Pasumarthi, J. Chaudhuri, A. K. Singh, H. Nemade, and D. Bandyopadhyay, "Self-spinning nanoparticle laden micro-droplets for sensing and energy harvesting," *Nanoscale*, vol. 8, no. 11, pp. 6118–6128, 2016.

[17] M. Bhattacharjee, A. Vilouras, and R. S. Dahiya, "Microdroplet-based organic vapour sensor on a disposable GO-chitosan flexible substrate," *IEEE Sensors J.*, vol. 20, no. 14, pp. 7494–7502, Jul. 2020.

[18] N. Mandal, M. Bhattacharjee, A. Chattopadhyay, and D. Bandyopadhyay, "Point-of-care-testing of α-amylase activity in human blood serum," *Biosens. Bioelectron.*, vols. 124–125, pp. 75–81, Jan. 2019.

[19] S. Thakur, M. Bhattacharjee, A. K. Dasmahapatra, and D. Bandyopadhyay, "Acoustic wave catalyzed urea detection utilizing a pulsatile microdroplet sensor," *ACS Sustain. Chem. Eng.*, vol. 7, no. 14, pp. 12069–12082, 2019.

[20] J. Kulys and E. J. D'Costa, "Printed electrochemical sensor for ascorbic acid determination," *Analytica Chimica Acta*, vol. 243, pp. 173–178, 1991.

[21] Y.-J. Hsu, Z. Jia, and I. Kymissis, "A locally amplified strain sensor based on a piezoelectric polymer and organic field-effect transistors," *IEEE Trans. Electron Devices*, vol. 58, no. 3, pp. 910–917, Mar. 2011.

[22] A. De Marcellis, C. Reig, and M.-D. Cubells-Beltrán, "A capacitance-to-time converter-based electronic interface for differential capacitive sensors," *Electronics*, vol. 8, no. 1, p. 80, 2019.

[23] A. Tsolis, W. G. Whittow, A. A. Alexandridis, and J. C. Vardaxoglou, "Embroidery and related manufacturing techniques for wearable antennas: Challenges and opportunities," *Electronics*, vol. 3, no. 2, pp. 314–338, 2014.

[24] Y. Wang *et al.*, "Flexible RFID tag metal antenna on paper-based substrate by inkjet printing technology," *Adv. Funct. Mater.*, vol. 29, no. 29, 2019, Art. no. 1902579.

[25] T. Leng, X. Huang, K. Chang, J. Chen, M. A. Abdalla, and Z. Hu, "Graphene nanoflakes printed flexible meandered-line dipole antenna on paper substrate for low-cost RFID and sensing applications," *IEEE Antennas Wireless Propag. Lett.*, vol. 15, pp. 1565–1568, 2016.

[26] T. Rai, P. Dantes, B. Bahreyni, and W. S. Kim, "A stretchable RF antenna with silver nanowires," *IEEE Electron Device Lett.*, vol. 34, no. 4, pp. 544–546, Apr. 2013.

[27] S. Khan, L. Lorenzelli, and R. S. Dahiya, "Technologies for printing sensors and electronics over large flexible substrates: A review," *IEEE Sensors J.*, vol. 15, no. 6, pp. 3164–3185, Jun. 2015.

[28] G. Yang, G. Pang, Z. Pang, Y. Gu, M. Mäntysalo, and H. Yang, "Non-invasive flexible and stretchable wearable sensors with nano-based enhancement for chronic disease care," *IEEE Rev. Biomed. Eng.*, vol. 12, pp. 34–71, Dec. 2018.

[29] M. Bhattacharjee, H. B. Nemade, and D. Bandyopadhyay, "Nano-enabled paper humidity sensor for mobile based point-of-care lung function monitoring," *Biosens. Bioelectron.*, vol. 94, pp. 544–551, Aug. 2017.

[30] R. Dahiya, "E-Skin: From humanoids to humans," *Proc. IEEE*, vol. 107, no. 2, pp. 247–252, Feb. 2019.

[31] J. Costantine, Y. Tawk, S. E. Barbin, and C. G. Christodoulou, "Reconfigurable antennas: Design and applications," *Proc. IEEE*, vol. 103, no. 3, pp. 424–437, Mar. 2015.

[32] A. M. Mansour *et al.*, "Compact reconfigurable multi-size pixel antenna for cognitive radio networks and IoT environments," in *Proc. Loughborough Antennas Propag. Conf. (LAPC)*, Loughborough, U.K., Nov. 2016, pp. 1–5.

[33] S. Ciccia, G. Giordanengo, and G. Vecchi, "Energy efficiency in IoT networks: Integration of reconfigurable antennas in ultra low-power radio platforms based on system-on-chip," *IEEE Internet Things J.*, vol. 6, no. 4, pp. 6800–6810, Aug. 2019.

[34] A. M. Mansour, N. Shehata, B. M. Hamza, and M. R. M. Rizk, "Efficient design of flexible and low cost paper-based inkjet-printed antenna," *Int. J. Antennas Propag.*, vol. 2015, Sep. 2015, Art. no. 845042.

[35] B. S. Cook and A. Shamim, "Utilizing wideband AMC structures for high-gain inkjet-printed antennas on lossy paper substrate," *IEEE Antennas Wireless Propag. Lett.*, vol. 12, pp. 76–79, 2013.

[36] B. I. Morshed, B. Harmon, M. S. Zaman, M. J. Rahman, S. Afroz, and M. Rahman, "Inkjet Printed Fully-Passive Body-Worn Wireless Sensors for Smart and Connected Community (SCC)," *J. Low Power Electron. Appl.*, vol. 7, no. 4, p. 26, 2017.

[37] R. Colella and L. Catarinucci, "Wearable UHF RFID sensor-tag based on customized 3D-printed antenna substrates," *IEEE Sensors J.*, vol. 18, no. 21, pp. 8789–8795, Nov. 2018.

[38] S. Kim, A. Georgiadis, and M. M. Tentzeris, "Design of inkjet-printed RFID-based sensor on paper: Single- and dual-tag sensor topologies," *Sensors*, vol. 18, no. 6, p. 1958, 2018.

[39] F. M. Tchafa and H. Huang, "Microstrip patch antenna for simultaneous strain and temperature sensing," *Smart Mater. Struct.*, vol. 27, no. 6, 2018, Art. no. 065019.

[40] J. Kim *et al.*, "Wearable smart sensor systems integrated on soft contact lenses for wireless ocular diagnostics," *Nat. Comm.*, vol. 8, no. 1, 2017, Art. no. 14997.

[41] H. Huang, "Flexible wireless antenna sensor: A review," *IEEE Sensors J.*, vol. 13, no. 10, pp. 3865–3872, Oct. 2013.

[42] H. Niu and R. D. Lorenz, "Evaluating different implementations of online junction temperature sensing for switching power semiconductors," *IEEE Trans. Ind. Appl.*, vol. 53, no. 1, pp. 391–401, Jan./Feb. 2017.

[43] H. K. Lee *et al.*, "Zinc oxide nanowire-based pressure and temperature sensor," in *Proc. 15th IEEE Int. Conf. Nanotechnol. (IEEE-NANO)*, Rome, Italy, Jul. 2015, pp. 901–904.

[44] Q. Liu, H. Tai, Z. Yuan, Y. Zhou, Y. Su, and Y. Jiang, "A high-performances flexible temperature sensor composed of polyethyleneimine/reduced graphene oxide bilayer for real-time monitoring," *Adv. Mater. Technol.*, vol. 4, no. 3, 2019, Art. no. 1800594.

[45] S. He, M. M. Mench, and S. Tadigadapa, "Thin film temperature sensor for real-time measurement of electrolyte temperature in a polymer electrolyte fuel cell," *Sens. Actuat. A, Phys.*, vol. 125, no. 2, pp. 170–177, 2006.

[46] Y. Zhang and Y. Cui, "Development of flexible and wearable temperature sensors based on PEDOT:PSS," *IEEE Trans. Electron Devices*, vol. 66, no. 7, pp. 3129–3133, Jul. 2019.

[47] B. B. Maskey *et al.*, "Proving the robustness of a PEDOT:PSS-based thermistor via functionalized graphene oxide–poly(vinylidene fluoride) composite encapsulation for food logistics," *RSC Adv.*, vol. 10, no. 21, pp. 12407–12414, 2020.

[48] P. Escobedo, M. Bhattacharjee, F. Nikbakhtnasrabadi, and R. Dahiya, "Smart bandage with wireless strain and temperature sensors and battery-less NFC tag," *IEEE Internet Things J.*, early access, Dec. 30, 2020, doi: 10.1109/JIOT.2020.3048282.

[49] A. Rivadeneyra *et al.*, "Cost-effective PEDOT:PSS temperature sensors inkjetted on a bendable substrate by a consumer printer," *Polymers*, vol. 11, no. 5, p. 824, 2019.

[50] R. Bhattacharyya, C. D. Leo, C. Floerkemeier, S. Sarma, and L. Anand, "RFID tag antenna based temperature sensing using shape memory polymer actuation," in *Proc. IEEE SENSORS*, Waikoloa, HI, USA, Nov. 2010, pp. 2363–2368.

[51] Y. Shafiq, S. V. Georgakopoulos, H. Kim, C. P. Ambulo, and T. H. Ware, "A patch antenna with liquid crystal elastomer switching for passive RFID temperature sensing," in *Proc. IEEE Int. Symp. Antennas Propag. USNC-URSI Radio Sci. Meeting*, Atlanta, GA, USA, Jul. 2019, pp. 1891–1892.

[52] S. Vihodceva, A. Ramata-Stunda, and A. Pumpure, "Evaluation of dermal toxicity of antibacterial cotton textile coated by sol-gel technology," *J. Textile Inst.*, vol. 109, no. 7, pp. 961–966, 2018.

[53] T. Zandt, H. Dwelk, C. Janowitz, and R. Manzke, "Quadratic temperature dependence up to 50 K of the resistivity of metallic $MoTe_2$," *J. Alloys Comp.*, vol. 442, nos. 1–2, pp. 216–218, 2007.

[54] W. L. Stutzman and G. A. Thiele, *Antenna Theory & Design*. New York, NY, USA: Wiley, 2012.

[55] C. A. Balanis, *Antenna Theory: Analysis and Design*. Chicester, U.K.: Wiley, 2012.

Mitradip Bhattacharjee (Member, IEEE) received the B.Tech. degree in electronics and communication engineering from the National Institute of Technology, Agartala, India, in 2013, and the Ph.D. degree from Indian Institute of Technology Guwahati, Guwahati, India, in 2018.

He is currently an Assistant Professor with the Electrical Engineering and Computer Science Department, Indian Institute of Science Education and Research, Bhopal, India. Subsequently, he joined the Bendable Electronics and Sensing Technologies Research Group, University of Glasgow, Glasgow, U.K., as a Postdoctoral Fellow in January 2019. His research interests include electronic sensors and systems, biomedical engineering, bioelectronics, flexible/printed and wearable electronics, wireless systems, and reconfigurable sensing antenna.

Fatemeh Nikbakhtnasrabadi (Graduate Student Member, IEEE) received the B.Sc. degree in electrical engineering and the M.Sc. degree in telecommunication engineering from Shahed University, Tehran, Iran, in 2010 and 2013, respectively. She is currently pursuing the Ph.D. degree with the BEST Group, University of Glasgow, Glasgow, U.K.

Her current research interests include designing antenna and RFID for healthcare application and smart labelling.

Ravinder Dahiya (Fellow IEEE) received the Ph.D. degree in humanoid technologies from the University of Genoa, Genoa, Italy, and Istituto Italiano di Tecnologia, Genoa, in 2009.

He is a Professor of Electronics and Nanoengineering with the University of Glasgow, Glasgow, U.K., where he is the Leader of Bendable Electronics and Sensing Technologies Research Group. He has authored over 350 research articles, seven books, and 15 submitted/granted patents. He has led several international projects. His group conducts fundamental and applied research in flexible and printable electronics, tactile sensing, electronic skin, robotics, and wearable systems.

Prof. Dahiya has received several awards, including the 2016 Microelectronic Engineering Young Investigator Award (Elsevier), the 2016 Technical Achievement Award from the IEEE Sensors Council, and 9 best paper awards as author/coauthor in international conferences and journals. He was a President-Elect from 2020 to 2021 and a Distinguished Lecturer of the IEEE Sensors Council and is serving on the editorial boards of the Scientific Report. He was also on the editorial boards of IEEE SENSORS JOURNAL from 2012 to 2020 and IEEE TRANSACTIONS ON ROBOTICS from 2012 to 2017. He was the Technical Program Co-Chair of IEEE Sensors 2017 and IEEE Sensors 2018 and has been the General Chair of several conferences, including IEEE FLEPS in 2019, 2020, and 2021, which he founded in 2019. He holds the prestigious EPSRC Fellowship and received in past the Marie Curie and Japanese Monbusho Fellowships.